PHYSICAL REVIEW D VOLUME 4, NUMBER 11 1 DECEMBER 1971

5-GeV/c Pion-Nucleon Scattering at All Angles*

Shu-Yuan Chu and Archibald W. Hendry
Physics Department, Indiana University, Bloomington, Indiana 47401
(Received 3 September 1971)

We fit all $\pi^{\pm}p$ elastic and charge-exchange data at 5 GeV/c on the basis of a simple geometric s-channel model.

I. INTRODUCTION

This paper is a continuation of an investigation into particle scattering processes at all angles, based on a particular s-channel model[1] suggested some time ago by the authors. The model was originally designed to account for the three prominent features that occur in the differential cross section of π^-p charge-exchange (CEX) scattering, namely, the dips at $t=0$ and -0.6 (GeV/c)^2 near the forward direction, and at $u=-0.2$ (GeV/c)^2 near the backward direction. By considering expansions of s-channel helicity amplitudes[2] in terms of d functions, it was shown[1] how these three features could be correlated if most of the scattering in this process came from a dominant band of angular momentum states centered around $j_c+\frac{1}{2}=kb_c$, where k is the c.m. momentum. In order for the CEX dips to occur at these places for all (intermediate) energies, the distance b_c had to be energy-independent, and it was estimated to be about 1 F.

As a first quantitative test of the model, we investigated[3] the case of π^+p elastic scattering for momenta $p_{\text{lab}}=2.74$, 3.0, 3.5, and 4.0 GeV/c. At these momenta, the differential cross sections have been measured *at all angles*; polarizations have been measured near the forward and backward directions; the total cross sections and the ratio of the real to the imaginary part of the nonflip amplitude at $t=0$ are also known. Fitting all of these quantities at any one energy provides a stringent test of the model, and our results were consistent with the general qualitative picture previously outlined for CEX scattering. We refer the reader to Ref. 3 for details. Here we remark only that the scattering was dominated by two main contributions:

(a) Diffraction, due to the absorption of the lower partial waves. It was shown that absorption was substantial (about 50%) for all partial waves corresponding to impact parameter $b\lesssim 0.8$ F, at which distance the absorption fell off rapidly to zero.

(b) Surface effects, at the edge of the interaction region. The angular momenta of these surface waves were indeed found to be centered around $j_c+\frac{1}{2}=kb_c$ with $b_c\approx 0.8$ F at all energies. The fact that b_c occurs at precisely the place where the absorption falls off clearly indicates the consistency of the model.

In the present paper, we extend the model further and examine simultaneously the three coupled reactions π^+p elastic scattering, π^-p elastic scattering, and π^-p CEX scattering at 5 GeV/c, since data have recently become available on these processes for scattering at all angles at approximately this energy. In the next section, Sec. II, we shall discuss our parametrization, our choice being guided in part by various Regge considerations. In Sec. III we list the experimental data used. The actual fits to the data are presented in Sec. IV, as well as a discussion of how the experimental features are explained in this model. We end with a few brief remarks in Sec. V.

II. PARAMETRIZATION: SUGGESTIONS FROM THE REGGE MODEL

In our previous investigation[3] of π^+p elastic scattering, we parametrized the low partial waves by Gaussians in j, and the peripheral band of angular momentum states by a single Breit-Wigner (BW) term in j. The latter form is also a simple Regge pole in the angular momentum plane for the s-channel reaction; such a form arises[4] naturally in all classical considerations of grazing rays. However, we found that a single Breit-Wigner term becomes less adequate as the energy is increased. The reason for this lies in the fact that, with a single BW term the sharp valley at $u=-0.2$ (GeV/c)^2 near the backward direction demands the BW width to be narrow; but this in turn leads to difficulties in canceling the resulting oscillations at intermediate angles in order to make the differential cross sections small there.

A modified parametrization is therefore adopted in the present paper, one that is suggested from considerations of the familiar Regge model (with duality). The latter model is of course applicable

only at the extreme edges of the scattering region; however, we try to extract some essential features and use them in our characterization of scattering at all angles from an s-channel point of view.

Let us consider typical Regge terms and expand them by a partial-wave analysis. For t-channel exchanges, we have

$$-s^{\alpha(t)}=\sum_{l=0}^{\infty}(2l+1)a_l(s)P_l(\cos\theta_s)\,, \tag{1}$$

$$-e^{-i\pi\alpha(t)}s^{\alpha(t)}=\sum_{l=0}^{\infty}(2l+1)c_l(s)P_l(\cos\theta_s)\,, \tag{2}$$

where

$$a_l=-s^{\alpha_0}e^{-y}(-i)^l j_l(iy)\,,$$

$$c_l=-e^{-i\pi\alpha_0}s^{\alpha_0}e^{(ix-y)}(-i)^l j_l(x+iy)\,,$$

and $\alpha(t)=\alpha_0+\alpha' t$, $x=2\pi\alpha' k^2$, $y=2\alpha' k^2\ln s$, and $j_l(z)$ is a spherical Bessel function. Now in the Veneziano model,[5] the nonrotating Regge term $s^{\alpha(t)}$ is constructed from the t- and u-channel resonances, while the rotating part $e^{-i\pi\alpha(t)}s^{\alpha(t)}$ corresponds to s- and t-channel resonances. Hence it is natural to associate[6] the $s^{\alpha(t)}$ term with the real nonresonating background in the s channel. In fact, $(-i)^l j_l(iy)$ for fixed large argument, behaves[7] very much like a Gaussian in l, stressing those partial waves with impact parameter $b=l/k \lesssim 0.8$ F. The rotating Regge part corresponds to s-channel resonances and is naturally associated with an s-channel Breit-Wigner term in angular momentum, like the one described above. [For a more detailed investigation of the connection between the Regge model (including cuts) and the present s-channel model, see Ref. 8.]

For u-channel exchanges, the expansions of $s^{\alpha(u)}$ and $e^{-i\pi\alpha(u)}s^{\alpha(u)}$ are similar, apart from an extra factor of $(-1)^l$. The importance of this latter factor becomes obvious when one remembers that in the backward direction the accompanying Legendre polynomials likewise alternate in sign with l. The $(-1)^l$ is therefore significant in building up structue in the backward direction. The presence of a $(-1)^l$ term brings about a distinction between even and odd partial waves, just like an exchange force in potential scattering, and leads to the breaking of "exchange degeneracy" in the s channel.

With these Regge forms and their s-channel partial-wave expansions in mind, we turn to our new parametrization of the s-channel helicity-nonflip and -flip amplitudes,[2]

$$f^s_{++}=\frac{1}{k}\sum(j+\tfrac{1}{2})T^j_{++}d^j_{1/2,1/2}(\theta_s)\,, \tag{3}$$

$$f^s_{+-}=\frac{1}{k}\sum(j+\tfrac{1}{2})T^j_{+-}d^j_{-1/2,1/2}(\theta_s)\,. \tag{4}$$

The T-matrix angular momentum elements T^j_{++}, T^j_{+-} were taken in the following form, for each isospin state $I=\frac{3}{2},\frac{1}{2}$:

$$T^j_{++}=F^R+iF^I+c_1G_L+(c_2+ic_3)G_{co}\times\mathrm{BW}\,, \tag{5}$$

$$T^j_{+-}=c_4G_L+(c_5+ic_6)G_{co}\times\mathrm{BW}\,. \tag{6}$$

We now explain the various pieces.

F^R and F^I are Fermi distributions (suggested from our previous π^+p analysis)[9]

$$F=\frac{f_1}{1+\exp[(b-f_2)/f_3]}$$

with $b=(j+\frac{1}{2})/k$. These represent the contribution from diffraction scattering (and hence are related to Pomeranchukon $I^t=0$ exchange), and are taken to be the same in both isospin states $I^s=\frac{3}{2},\frac{1}{2}$. We would anticipate f_2 to be about 0.8 F. (F^R, F^I: six parameters.)

Each coefficient c_i is of the form $c=d+(-1)^l e$, a reflection of the expansions of t- and u-channel Regge terms. ($c_i^{3/2}$, $c_i^{1/2}$: 24 parameters.)

G_L is a Gaussian,

$$G_L=\exp(-g_L b^2)\,,$$

and is the real low-partial-wave contribution corresponding to s^α. [As already mentioned, $(-1)^l j_l(iy)$ behaves like a Gaussian as a function of l.]

G_{co} is a smooth cutoff function

$$G_{co}=\exp[-g_{co}(b-b_c)^2]$$

for the Breit-Wigner s-channel Regge pole

$$\mathrm{BW}=\frac{\Gamma/2}{k(b-b_c)-i\Gamma/2}\,.$$

This represents the scattering from the edge of the interaction region (or, alternatively, the rotating Regge part). G_L, G_{co}, and BW are taken to be the same in both isospin states $I^s=\frac{3}{2},\frac{1}{2}$ and it was found sufficient to take $g_L=g_{co}=g$. (G_L, G_{co}, and BW: three parameters.)

Altogether there are 33 parameters to describe π^+p elastic scattering, π^-p elastic scattering and π^-p CEX scattering at all angles. We have not attempted to obtain a fit with some minimum number of parameters. What we have done is to use a parametrization whose pieces are clearly interpretable.

III. DATA

The data used in the fitting were the following:

Differential Cross Section ($d\sigma/dt$)

$\pi^\pm p$ elastic: Brabson *et al.*[10] (Indiana);
Chandler *et al.*[11] (Indiana);
Rust *et al.*[12] (Argonne-NAL-Michigan);
Coffin *et al.*[13] (Michigan).

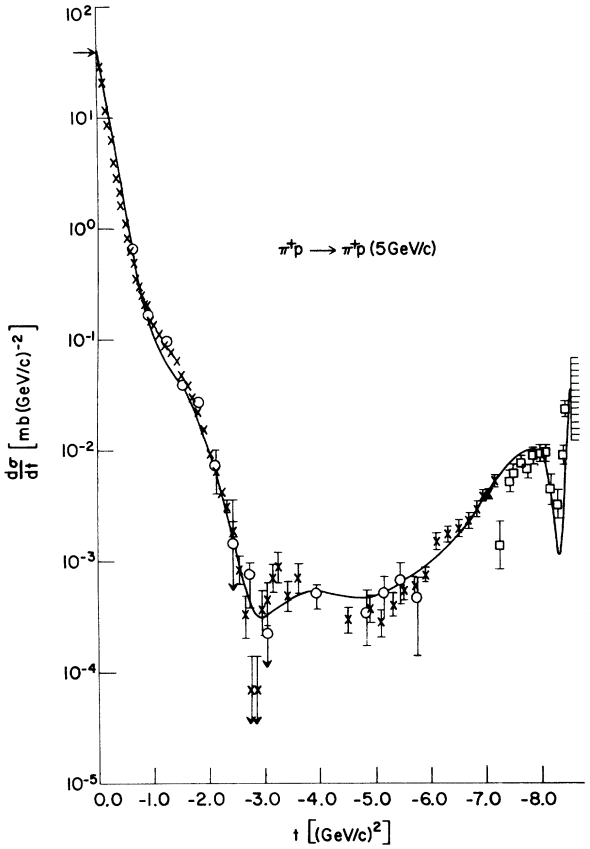

FIG. 1. π^+p differential cross section; see Sec. III for data.

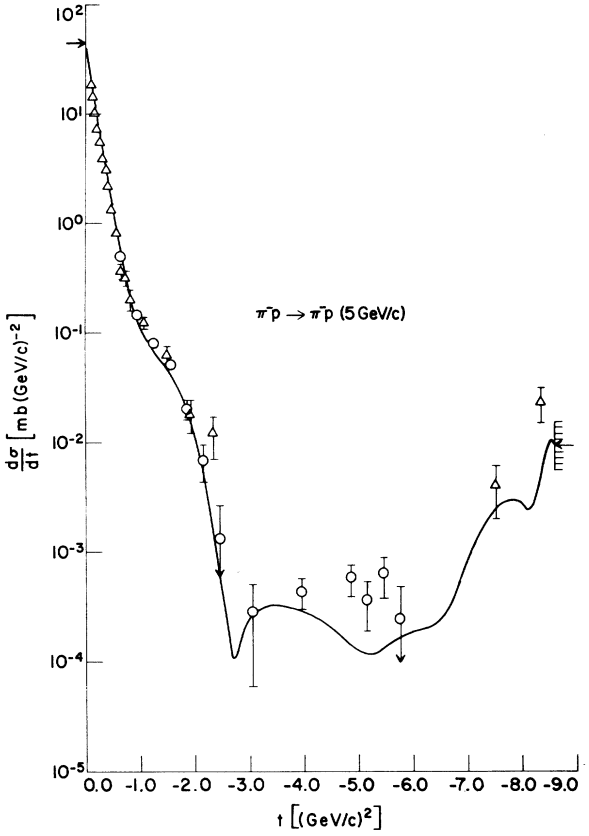

FIG. 2. π^-p differential cross section; see Sec. III for data.

The π^-p 180° point comes from Kormanyos *et al.*[14] (Michigan-Argonne).

π^-p CEX: Yvert[15];
Chase *et al.*[16] (Minnesota);
Brockett *et al.*[17] (Case Western-Oberlin), 4.83 GeV/c.

Polarizations

π^+p elastic: Esterling *et al.*[18] (Chicago-Argonne), 5.15 GeV/c.

π^-p elastic: Esterling *et al.*[18] (Chicago-Argonne), 5.15 GeV/c.

π^-p CEX: Drobnis *et al.*[19] (Argonne).

All the amplitudes at $t=0$ have been calculated by Höhler and Strauss[20] from forward dispersion relations. At 5 GeV/c, they estimate

$$\sigma_{tot}(\pi^+p) = 26.61 \text{ mb},$$

$$\sigma_{tot}(\pi^-p) = 28.97 \text{ mb},$$

$$\mathrm{Re}f_{++}(\pi^+p)/\mathrm{Im}f_{++}(\pi^+p) = -0.29 \text{ at } t=0,$$

$$\mathrm{Re}f_{++}(\pi^-p)/\mathrm{Im}f_{++}(\pi^-p) = -0.15 \text{ at } t=0.$$

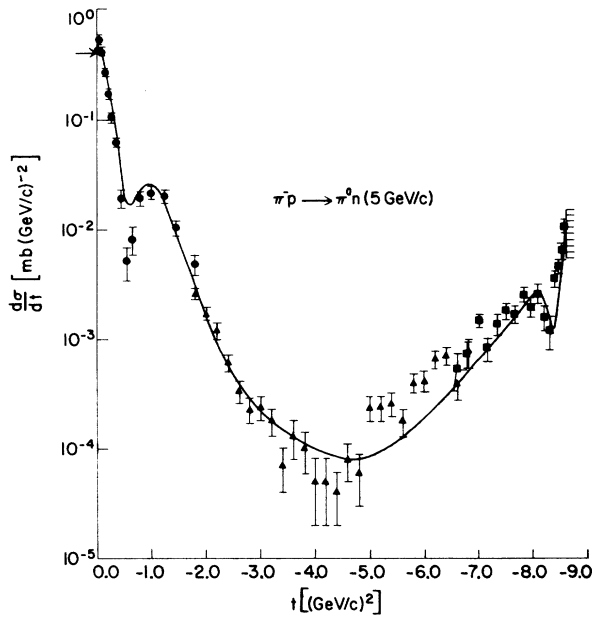

FIG. 3. π^-p CEX differential cross section; see Sec. III for data.

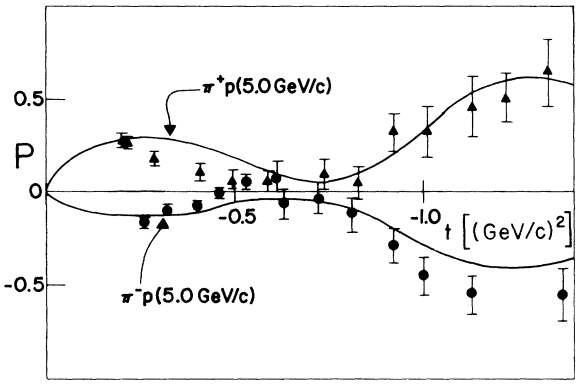

FIG. 4. $\pi^{\pm}p$ forward elastic polarizations; see Sec. III for data.

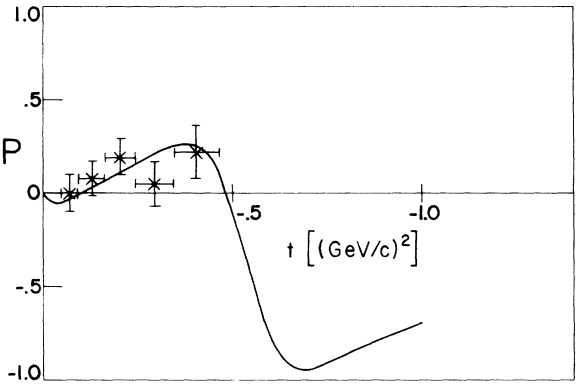

FIG. 5. π^-p CEX forward polarization; see Sec. III for data.

IV. FITS TO THE DATA; EXPLANATION OF EXPERIMENTAL FEATURES; STRUCTURE OF THE AMPLITUDES

Using the parametrization described in Sec. II, we obtained a fit to all the data available for pion-nucleon scattering at 5 GeV/c. The fits to the differential cross sections at all angles $0 \geq t \geq -8.57$ (GeV/c)^2 are shown in Figs. 1, 2, and 3, the $\pi^{\pm}p$ polarizations in Fig. 4, and the π^-p CEX polarization in Fig. 5. Our values of the total cross sections for $\pi^{\pm}p$ scattering were 27.2 and 29.6 mb, respectively, and the ratios of the real to imaginary parts of the forward nonflip amplitude were −0.29 and −0.15. The corresponding values of the parameters are listed in Table I.

We now go on to discuss how the main experimental features come about in our fits. For the sake of clarity, we have drawn in Figs. 6, 7, and 8 the s-channel helicity amplitudes at all angles for π^+p elastic scattering, π^-p elastic scattering, and π^-p CEX scattering, respectively. These are related to the s-channel isospin $I^s = \frac{3}{2}, \frac{1}{2}$ and the t-channel isospin $I^t = 0$, 1 amplitudes by

$$f(\pi^+p) = f^{3/2} = f^0 - f^1 ,$$
$$f(\pi^-p) = \tfrac{1}{3}(f^{3/2} + 2f^{1/2}) = f^0 + f^1 ,$$
$$f(\mathrm{CEX}) = \tfrac{1}{3}\sqrt{2}\,(f^{3/2} - f^{1/2}) = -\sqrt{2}\,f^1 .$$

A. Forward $\pi^{\pm}p$; $0 \geq t \geq -1.5$ (GeV/c)^2

The forward elastic peak and subsequent shoulder are due primarily to diffraction, originating from the absorption of the lower partial waves. In Fig. 9, we have drawn the corresponding Fermi distributions F^R, F^I (which are the same for $I^s = \frac{3}{2}, \frac{1}{2}$ and hence are pure $I^t = 0$) as functions of the impact parameter b. From F^I, we see that the absorption is substantial for all partial waves with $b \lesssim 0.8$ F, at which distance it falls off quite rapidly to zero.

It should be noted[21] that the imaginary part of f^s_{++}, which dominates in the forward peak itself, has a zero at $t = -0.7$ (GeV/c)^2, the resulting hole in $d\sigma/dt$ being filled up by the real part of f^s_{++}. This is quite different from the usual Regge parametrization of diffraction where the Pomeran-

TABLE I. Parameter values. All parameters are in units of ($\sqrt{\text{mb}}$ GeV), except f_2 and b_c, which are in fermis, and $\Gamma/2$ is dimensionless.

	f_1	f_2	f_3
F^R	−0.21	0.63	0.80
F^I	0.33	0.75	0.71

	g	b_c	$\Gamma/2$
BW	0.21	0.93	6.0

Coefficients c	d_1	e_1	d_2	e_2	d_3	e_3	d_4	e_4	d_5	e_5	d_6	e_6
$I^s_- = \frac{3}{2}$	−0.101	−0.038	0.054	0.002	−0.026	−0.005	−0.001	−0.001	0.021	0.002	−0.026	0.008
$I^s = \frac{1}{2}$	−0.019	−0.006	0.084	0.007	0.049	−0.003	0.012	−0.012	−0.028	0.003	0.028	−0.003

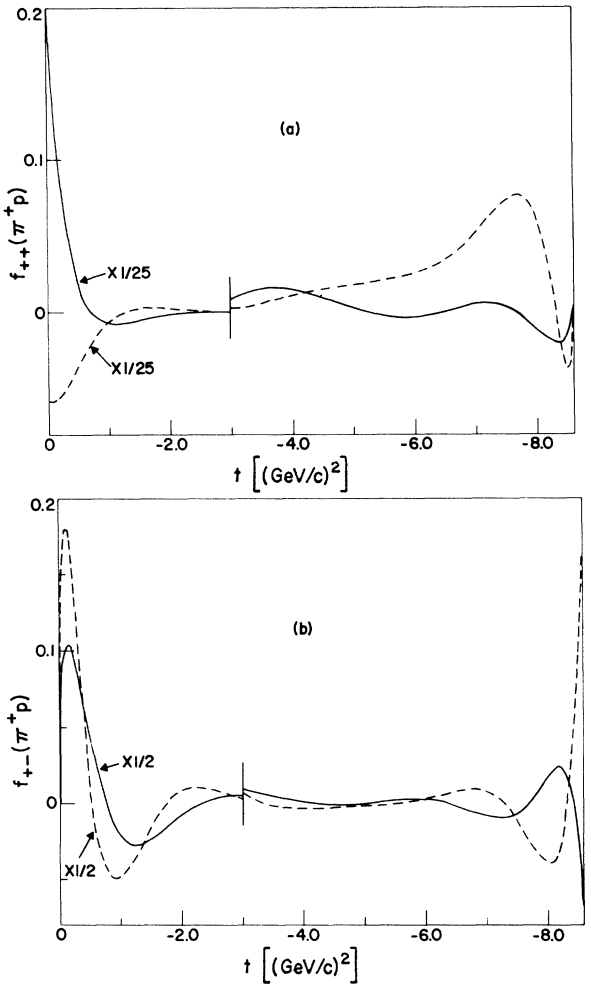

FIG. 6. Real (dashed line) and imaginary (solid line) parts of π^+p s-channel (a) helicity-nonflip, (b) helicity-flip amplitudes (in $\sqrt{\text{mb}}$). In the forward directions, the amplitudes have been reduced by the factors indicated.

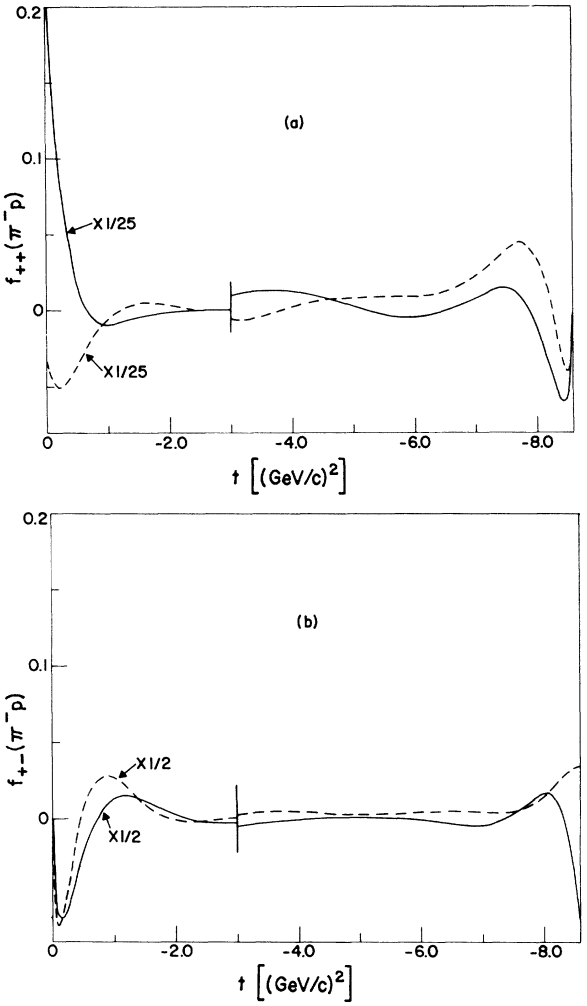

FIG. 7. Real (dashed line) and imaginary (solid line) parts of π^-p s-channel (a) helicity-nonflip, (b) helicity-flip amplitudes (in $\sqrt{\text{mb}}$).

chukon[22] is taken to be structureless, i.e., no zeros. Also in Harari's recent "dual-absorptive" model,[23] Pomeranchukon diffraction is taken to be structureless, the sudden change of slope in $d\sigma/dt$ at $t \approx -0.8$ (GeV/c)^2 being due in his model to interference with direct-channel resonances.

This point as to whether the imaginary part of the nonflip amplitude has a diffraction zero at $t \approx -0.7$ (GeV/c)^2 or not is an important distinction between the two types of models. In particular, the explanation of the double zero of the π^+p polarizations at $t = -0.6$ (GeV/c)^2 (see below) is different.

B. Crossover at $t=-0.2$ (GeV/c)^2

The crossover point at $t = -0.2$ (GeV/c)^2 of the $\pi^\pm p$ elastic differential cross sections arises from the zero in the imaginary part [see Fig. 8(a)] of the s-channel helicity nonflip amplitude in the CEX reaction. Regge fits also have a zero here in this amplitude,[22] but it is written in initially as a multiplicative factor in the parametrization. In the present model, it is easy to see how it comes about naturally from the BW term in (5) and the property that $d^{j_c}_{1/2,1/2}(\theta_s) \approx J_0(b_c\sqrt{-t})$ has a zero at $t \approx -0.2$ (GeV/c)^2 for $b_c \approx 0.9$ F.

C. CEX dips at $t=-0.6$ (GeV/c)^2 and $u=-0.2$ (GeV/c)^2

The qualitative correlation of these dips provided the original motivation[1] of the model, as discussed in the Introduction. Our present fits support the original proposal, namely, that they come

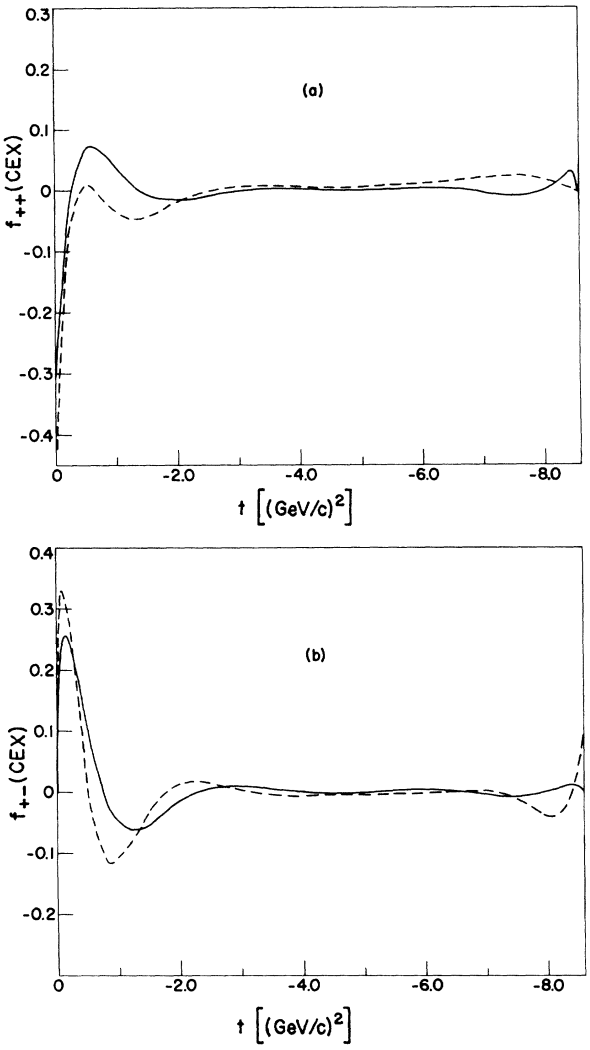

FIG. 8. Real (dashed line) and imaginary (solid line) parts of $\pi^- p$ CEX s-channel (a) helicity-nonflip, (b) helicity-flip amplitudes (in $\sqrt{\text{mb}}$).

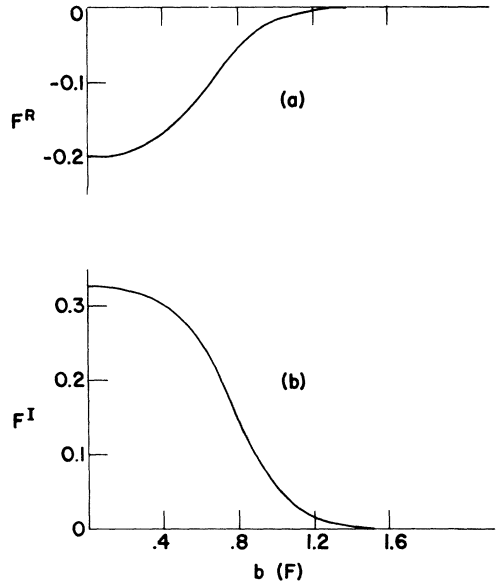

FIG. 9. Partial-wave composition (in $\sqrt{\text{mb}}$ GeV) of (a) F^R, (b) F^I against impact parameter b in fermis.

about in a unified way primarily from the peripheral angular momentum band (parametrized here by a BW term) in the flip amplitude. To illustrate this point further, we show in Fig. 10 the contribution of the s-channel helicity-flip CEX BW term, and in Fig. 11 the partial-wave decomposition of this BW term. The BW curve is centered around $b \approx 0.9$ F, and clearly gives rise to the experimental structure at $t = -0.6$ (GeV/c)^2 and $u = -0.2$ (GeV/c)^2, as anticipated.

The $u = -0.2$ (GeV/c)^2 dip in backward $\pi^+ p$ elastic scattering originates in a similar way. In backward $\pi^- p$ elastic scattering, the precise shape is not well determined, due to the lack of good data in this region.

D. Polarization at $t = -0.6$ (GeV/c)^2

The dips in the elastic $\pi^\pm p$ polarization around $t = -0.6$ (GeV/c)^2 suggest a double zero. In the present model, one zero comes from the vanishing of the imaginary part of the s-channel helicity-nonflip amplitude [see Figs. 6(a) and 7(a)] at $t \approx -0.7$ (GeV/c)^2 (the same zero that produces the first diffraction zero in the elastic differential cross sections). The other zero comes from a zero in the real part of the s-channel helicity-flip amplitude [see Figs. 6(b) and 7(b)] at $t \approx -0.5$ (GeV/c)^2. The approximate mirror symmetry of the forward $\pi^\pm p$ polarizations comes from the fact that the real parts of the $\pi^\pm p$ flip amplitudes are of opposite sign (in Regge language, this corresponds to saying that the real part of this flip amplitude is dominated by the $I^t = 1$ exchange contribution).

We note that the explanation of these polarization structures is different from the usual Regge explanation. There, the double zero comes from the real part of the signature term for ρ exchange (the Pomeranchukon being structureless). In the present approach, it is more natural to have just a single zero in the real part of the flip amplitude [arising from the oscillations of the $d^J_{-1/2,1/2}(\theta_s)$ function].

In our fit, the $\pi^- p$ CEX polarization has a simple zero around $t = -0.5$ (GeV/c)^2. [Since this work was completed, recent (as yet unpublished) CERN CEX polarization measurements[24] at 5 and

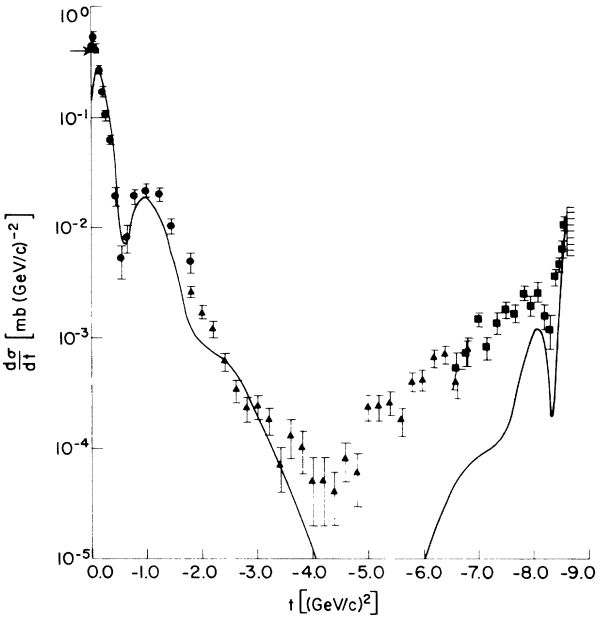

FIG. 10. Contribution of peripheral Breit-Wigner term in s-channel helicity-flip amplitude to CEX differential cross section.

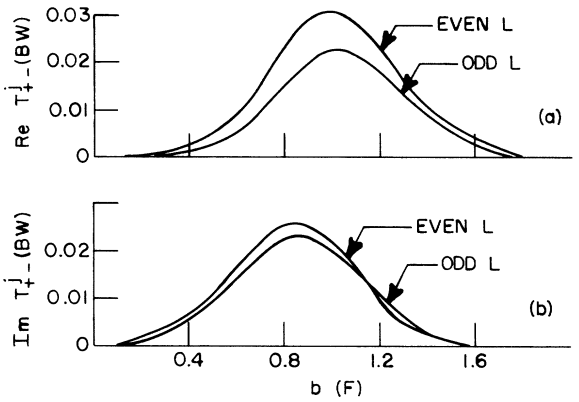

FIG. 11. Partial-wave composition (in $\sqrt{\text{mb}}$ GeV) of (a) real part, (b) imaginary part of the s-channel helicity-flip BW term in CEX scattering, against impact parameter b (F).

8 GeV/c have become available. At 5 GeV/c the polarizations for small t are considerably more positive than those of Ref. 19 used in the present fit; although the error bars are still large, there is an indication of a single zero around $t = -0.8$ (GeV/c)^2. The 8-GeV/c data are certainly consistent with having a single zero around $t = -0.5$ (GeV/c)^2. We hope to include these latest data in subsequent fitting.]

V. CONCLUDING REMARKS

We have demonstrated that it is possible to obtain a reasonable fit to all the pion-nucleon scattering data at 5 GeV/c. We find that the data *at all angles* can be correlated on the basis of a straightforward s-channel geometric picture,[1] that of scattering from an absorbing interaction region of radius about 0.8–0.9 F and at the edge of which there are strong edge effects.

*Work supported in part by the U. S. Atomic Energy Commission under Contract No. AT(11-1)-2009B.

[1]S. Y. Chu and A. W. Hendry, Phys. Rev. Letters 25, 313 (1970).

[2]M. Jacob and G. C. Wick, Ann. Phys. (N.Y.) 1, 404 (1959).

[3]S. Y. Chu and A. W. Hendry, Phys. Rev. D 4, 2743 (1971).

[4]R. G. Newton, *Scattering Theory of Waves and Particles* (McGraw-Hill, New York, 1966).

[5]G. Veneziano, Nuovo Cimento 57A, 190 (1968).

[6]P. W. Coulter, E. S. Ma, and G. L. Shaw, Phys. Rev. Letters 23, 106 (1969).

[7]See, for instance, *Handbook of Mathematical Functions*, edited by M. Abramowitz and I. A. Stegun (U. S. Government Printing Office, Washington, D. C., 1964).

[8]A. W. Hendry, Phys. Rev. D (to be published).

[9]B. Kozlowsky and A. Dar, Phys. Letters 20, 311 (1966), used Fermi distribution in their "strong absorption model."

[10]B. B. Brabson, R. R. Crittenden, R. M. Heinz, R. C. Kammerud, H. A. Neal, H. W. Paik, and R. A. Sidwell, Phys. Rev. Letters 25, 253 (1970).

[11]J. P. Chandler, R. R. Crittenden, K. F. Galloway, R. M. Heinz, H. A. Neal, K. A. Potocki, W. F. Frickett, and R. A. Sidwell, Phys. Rev. Letters 23, 186 (1969).

[12]D. R. Rust, P. N. Kirk, R. A. Lundy, C. E. W. Ward, D. D. Yovanovitch, S. M. Pruss, C. W. Akerlof, K. S. Han, D. I. Meyer, and P. Schmueser, Phys. Rev. Letters 24, 1361 (1970).

[13]C. T. Coffin, N. Dikman, L. Ettlinger, D. Meyer, A. Sanlys, K. Terwilliger, and D. Williams, Phys. Rev. 159, 1169 (1967).

[14]S. W. Kormanyos, A. D. Krisch, J. R. O'Fallon, K. Ruddick, and L. G. Ratner, Phys. Rev. Letters 16, 709 (1966).

[15]Yvert *et al.* (unpublished); G. Giacomelli, P. Pini, and S. Stagni, CERN Report No. CERN-HERA 69-1 (unpublished).

[16]R. C. Chase, E. Coleman, H. W. J. Courant, E. Marquit, E. W. Petraske, H. F. Romer, and K. Ruddick, Phys. Rev. D 2, 2588 (1970).

[17]W. S. Brockett, G. T. Corlew, W. R. Frisken, T. L. Jenkins, A. R. Kirby, C. R. Sullivan, J. A. Todoroff,

and W. B. Richards, Phys. Rev. Letters 26, 527 (1971).
[18]R. J. Esterling, N. E. Booth, G. Conforto, J. Parry, J. Sheid, D. Sherden, and A. Yokosawa, Phys. Rev. Letters 21, 1410 (1968).
[19]D. D. Drobnis, J. Lales, R. C. Lamb, R. A. Lundy, A. Moretti, R. C. Niemann, T. B. Novey, J. Simanton, A. Yokosawa, and D. D. Yovanovitch, Phys. Rev. Letters 20, 274 (1968).
[20]G. Höhler and R. Strauss, University of Karlsruhe report (unpublished).
[21]See Ref. 3 for a similar discussion of this in the p_{lab} = 2.74–4.0 GeV/c range.
[22]Throughout the forward t range, the s-t helicity crossing matrix is approximately the diagonal unit matrix, so one can compare the s- and t-helicity amplitudes directly.
[23]H. Harari, Ann. Phys. (N.Y) 63, 432 (1971).
[24]CERN polarization group (unpublished).

PHYSICAL REVIEW D VOLUME 4, NUMBER 11 1 DECEMBER 1971

Polarization and Dip-Bump Structure in $\pi^- p$ Charge-Exchange Scattering

S. Kogitz and R. K. Logan
Physics Department, University of Toronto, Toronto 5, Ontario, Canada
(Received 19 July 1971)

We show that the new $\pi^- p$ charge-exchange polarization and differential cross-section data at large angles can be explained in terms of a simple model which includes a ρ Regge pole plus a background term which one may interpret as either a secondary pole or a cut. We show that the rise after the dip is primarily due to the background term and not the spin-flip Regge term recovering from α passing through zero near $t = -0.6$ GeV^2. We discuss the effect of this insight on dip systematics.

The first measurements[1,2] of $\pi^- p$ charge-exchange (CEX) scattering indicated[3] that this reaction is dominated by single-ρ-Regge-pole exchange. Subsequent measurements of polarization[4] indicated that another term is contributing, which some took as evidence for a second Regge pole, the ρ',[5-7] and others as evidence for a cut.[8,9] As there is no way of discerning which of these two models is correct on the basis of presently available experimental data, we plan to use here a simple model which includes the ρ Regge pole plus a background term which can be considered to be a secondary pole or cut depending on whether we parametrize the energy dependence of the background term with $(s/s_0)^{\alpha_{\rho'}}$ or $[\ln(s/s_0)]^{-1}$.

One of the interesting features of the differential cross section is the dip near $t = -0.6$ GeV^2 followed by a bump. This structure has been attributed to the fact that the α factor multiplying the spin-flip amplitude passes through zero near $t = -0.6$ GeV^2. Because of factorization one expects to see this same dip-bump structure in other reactions in which the ρ is exchanged, such as $\pi N \to \omega N$ or $\gamma N \to \pi N$. This is not always the case, however, and a great deal of attention has been given to explaining why a dip occurs for some reactions and not for others. Bander and Gotsman[10] correlate the presence or absence of a dip with an α^2 or α factor, respectively, claiming that $|\alpha^m \tilde{\beta} s^\alpha + f_{\text{BG}}|^2 \approx |f_{\text{BG}}|^2 + 2\alpha^m \tilde{\beta} s^\alpha f_{\text{BG}}$ near $\alpha = 0$ will only give a dip for $m = 2$. We have investigated this point further and showed that if both βs^α and f_{BG} are exponentially decaying in t, then no matter what power of α one uses one will not obtain a dip because the exponential t dependence of $\tilde{\beta} s^\alpha$ and f_{BG} wins out over the power behavior of α. It is our contention that the dip is due to the α factor but that the rise above the dip and the maximum near $t = -1$ GeV^2 are due primarily to the background term and not to the ρ spin-flip term recovering from α passing through zero. We have therefore considered a simple model incorporating this feature which, with a minimum of free parameters, can explain the present experimental data on $\pi^- p$ CEX scattering, including the very recent measurements at large angles of both the differential cross section[11] and the polarization.[12]

In our analysis we will make use of the amplitudes defined by Singh.[13] The differential cross section is given by

$$\frac{d\sigma(s,t)}{dt} = \frac{1}{\pi s}\left(\frac{M}{4k}\right)^2 \left| \left(1 - \frac{t}{4M^2}\right)|A'|^2 - \frac{t}{4M^2}\left(\frac{4M^2 p^2 + st}{4M^2 - t}\right)|B|^2 \right|, \tag{1}$$

the difference of the $\pi^- p$ and $\pi^+ p$ total cross sections by

$$\Delta\sigma_{\text{tot}}(s) = \sqrt{2}\,\text{Im}A'(s, t=0)/p\,, \tag{2}$$

and the polarization by